# Nuclear magnetic relaxation and electron-spin fluctuation in a triangular-lattice Heisenberg antiferromagnet $CsNiBr_3$

Satoru Maegawa
*Graduate School of Human and Environmental Studies, Kyoto University, Kyoto 606-01, Japan*
(Received 7 November 1994)

The spin-lattice relaxation time $T_1$ of $^{133}Cs$ in $CsNiBr_3$ has been measured to study the spin fluctuation in the triangular-lattice Heisenberg antiferromagnet with a small easy-axis anisotropy. This compound shows the successive phase transitions at $T_{N1}=14.06$ K and $T_{N2}=11.51$ K. The relaxation rate $T_1^{-1}$ in the paramagnetic phase is governed by the paramagnetic modulation of the exchange interaction. It is well explained by using the observed static susceptibility down to $T_{N1}$. The relaxation rate changes drastically at $T_{N1}$, and below this temperature the rates at inequivalent Cs sites become different from each other. The relaxation rate in the low-temperature phase below $T_{N2}$ has a strong temperature dependence, while it has no field dependence. This relaxation rate is well explained by the two-magnon (Raman) process due to the swinging fluctuation of the triangular spin structure in the $zx$ plane.

## I. INTRODUCTION

The magnetic properties of antiferromagnets on the triangular lattice have been attracting considerable attention because of the interest in the frustration effect. In these systems the antiferromagnetic interactions on the triangular lattice compete with each other and consequently give rise to phenomena such as successive magnetic phase transitions, a noncollinear ordered phase, and peculiar fluctuations.

The hexagonal $ABX_3$-type compound $CsNiBr_3$ is one of the typical Heisenberg antiferromagnets with a small easy-axis anisotropy on the triangular lattice. $CsNiBr_3$ belongs to the space group $P6_3/mmc$ with lattice parameters of $a=7.60$ Å and $c=6.50$ Å.[1] The $Ni^{2+}$ ions align along the hexagonal $c$ axis and these chains form the triangular structure in the basal $c$ plane. The interactions along the chain and in the plane are both antiferromagnetic, but the former interaction $J_0$ is much larger than the latter $J_1$. The electron-spin system is described by the Hamiltonian

$$H_e=2J_0\sum_{\langle i,j\rangle}^{\text{intra}}\mathbf{S}_i\cdot\mathbf{S}_j+2J_1\sum_{\langle i,k\rangle}^{\text{inter}}\mathbf{S}_i\cdot\mathbf{S}_k-D\sum_i(S_i^z)^2\ , \qquad (1)$$

where $S=1$, $J_0=17.0$ K,[2] and $J_1=0.31$ K.[3] The easy-axis anisotropy $D$ is estimated to be 0.65 K from the relation $D=(g\mu_B H_{SF})^2/16J_0S^2$ using the experimental values of the spin-flop field $H_{SF}=9.0$ T,[4] and $g=2.20$.[5] The $Cs^+$ ion is located at the center of a unit prism surrounded by six $Ni^{2+}$ ions. The antiferromagnetic interchain interaction and the small easy-axis anisotropy lead to characteristic ordered phases at low temperature. In previous work we have revealed the magnetic structures of the successively ordered phases by means of the NMR spectrum of $^{133}Cs$.[3] The results are summarized as follows. The antiferromagnet $CsNiBr_3$ undergoes two magnetic phase transitions at $T_{N1}=14.06$ K and $T_{N2}=11.51$ K. In the intermediate phase between $T_{N1}$ and $T_{N2}$ the component of the magnetic moments parallel to the $c$ axis orders and the moments form a collinear structure of cosine mode. In the low-temperature phase below $T_{N2}$ the component perpendicular to the $c$ axis also orders and the moments form a triangular structure in a plane including the $c$ axis, in which the moments in one-third of the chains are parallel to the $c$ axis and those in the remaining two-thirds cant from the $c$ axis at $\pm 39°$ The ratio $D/J_1$ was obtained to be 2.1. The isomorphic crystal $CsNiCl_3$ belongs to the same family with the Hamiltonian described by Eq. (1) and shows similar properties, but has a smaller $D/J_1$.[6]

In the present work we have measured the spin-lattice relaxation time $T_1$ of $^{133}Cs$ in $CsNiBr_3$ to study the dynamic behavior in the frustrated antiferromagnetic on the triangular lattice.

## II. EXPERIMENTAL PROCEDURE

Single crystals of $CsNiBr_3$ grown by the Bridgman method were used. The coherent pulsed NMR method was utilized with the operating frequencies of 2.0, 4.0, and 7.0 MHz. The spin-lattice relaxation times were obtained by measuring the spin-echo intensity as a function of the time interval between the saturation comb pulses and the two searching pulses. The measurements were performed in the temperature range between 1.5 and 77 K. The recoveries of the spin-echo intensity were single exponential as a function of time in the whole temperature range.

## III. EXPERIMENTAL RESULTS

At each measurement of $T_1$ the NMR spectrum of the $^{133}Cs$ nuclei was observed in advance by recording the spin-echo intensity as a function of the external field at a fixed frequency. In the paramagnetic phase above $T_{N1}$ the NMR spectrum has a single peak at the resonance field of a free $^{133}Cs$ nucleus. In the intermediate phase the NMR spectrum splits into plural peaks for $\mathbf{H}_0\perp c$ axis, while only one peak remains to be observed for $\mathbf{H}_0\|c$ axis. For $\mathbf{H}_0\perp c$ axis, three sharp peaks are observed for $\mathbf{H}_0\|a$ axis and four sharp peaks are observed for $\mathbf{H}_0\perp a$ and $c$ axes. In the low-temperature phase the features of the NMR spectrum do not change for $\mathbf{H}_0\perp c$ axis, while the

 

NMR spectrum spreads out and has a powder pattern for $\mathbf{H}_0 \| c$ axis in spite of the single crystal. The plural NMR peaks in the ordered phases correspond to the existence of six magnetically inequivalent Cs sites with different internal magnetic fields. The temperature and angular dependences of the resonance fields give information on the magnetic structure in each phase, and the results have been reported previously.[3] In the present work we have measured the relaxation times $T_1$ at each peak.

Figure 1 shows the temperature dependence of the relaxation rates $T_1^{-1}$ at the resonance frequency of 4.0 MHz between 1.5 and 77 K. In the paramagnetic phase $T_1^{-1}$ decreases slowly with decreasing temperature and there is no remarkable difference between the relaxation rates for $\mathbf{H}_0 \perp c$ axis and $\mathbf{H}_0 \| c$ axis. As the temperature is decreased across $T_{N1} = 14.06$ K, the NMR peak begins to split and $T_1^{-1}$ changes abruptly at each peak. We designate three peaks as $a_1$, $a_2$, and $a_3$ for $\mathbf{H}_0 \| a$ axis and four peaks as $b_1$, $b_2$, $b_3$, and $b_4$ for $\mathbf{H}_0 \perp a$ and $c$ axes in order of the magnitude of the resonance field. The central position of the peak for $\mathbf{H}_0 \| c$ axis is designated by $c$. The relaxation rates at these peaks are shown in Fig. 1. The temperature dependence of $T_1^{-1}$ below $T_{N1}$ is stronger than that in the paramagnetic phase. At $T_{N2}$ the relaxation rates change continuously, but $T_1^{-1}$ at $b_1$ and $c$ shows small bends of the temperature dependence, while that at $a_2$ peak shows a small cusp. The ratio of $T_1^{-1}$ at $b_1$ and at $a_2$ is about 8 in the intermediate phase, while it is about 1.5 in the low-temperature phase except for the transient temperature region near $T_{N2}$.

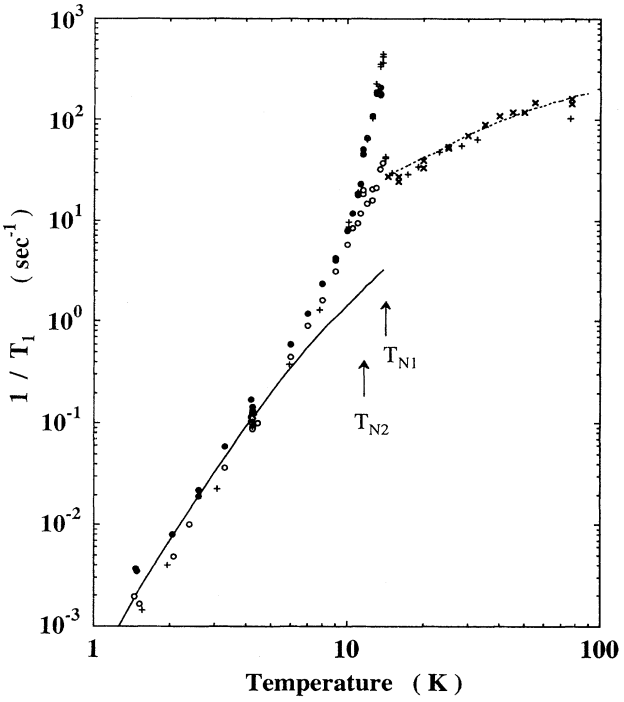


FIG. 1. Temperature variation of the relaxation rates $T_1^{-1}$ at 4.0 MHz. +: the relaxation rate at the central position of the $c$ peak for $H_0 \| c$ axis. ×: the rate in the paramagnetic phase for $H_0 \perp c$ axis. ●: the rate at the $b_1$ peak of the lowest resonance field among four peaks for $H_0 \perp c$ and $a$ axes in the ordered phases. ○: the rate at the central $a_2$ peak among three peaks for $\mathbf{H}_0 \| a$ axis. The broken curve indicates the calculated temperature dependence of the rate in the paramagnetic phase. The solid curve indicates the temperature dependence of the rate in the low-temperature phase calculated from Eq. (24).

The peak dependence of the relaxation rates for $\mathbf{H}_0 \perp c$ axis at 13.0 K in the intermediate phase and at 4.2 K in the low-temperature phase is shown in Fig. 2. The difference of the NMR peaks corresponds to that of the angle $\phi$ between the external field in the $c$ plane and the internal dipolar fields at the Cs sites.[3] In the intermediate phase the $Ni^{2+}$ moments are directed parallel to the $c$ axis and so the dipolar fields at the Cs sites lie in the $c$ plane, while in the low-temperature phase the noncollinear spin structure causes dipolar fields that have both parallel and perpendicular components to the $c$ axis. The relaxation rates at the $a_2$ and $b_1$ peaks correspond to the rates at which the external field is perpendicular and parallel, respectively, to the component of the dipolar field in the $c$ plane. As is found in Fig. 2, $T_1^{-1}$ is symmetric around $\phi = 90°$ in both phases. In the intermediate phase the $\phi$ dependence of $T_1^{-1}$ shows one minimum at $\phi = 90°$ ($a_2$ peak).

The spin-lattice relaxation rate is controlled by the transverse fluctuation of the local field at the nuclear site with respect to the external field. In the intermediate phase the site dependence is easily explained as follows. When we designate the intensity of the fluctuation component parallel to the static internal field in the $c$ plane as $h_1$, that of the component parallel to the $c$ axis as $h_3$, and that of the component perpendicular to both the internal field and the $c$ axis as $h_2$, the relaxation rate for $\mathbf{H}_0 \perp c$ axis

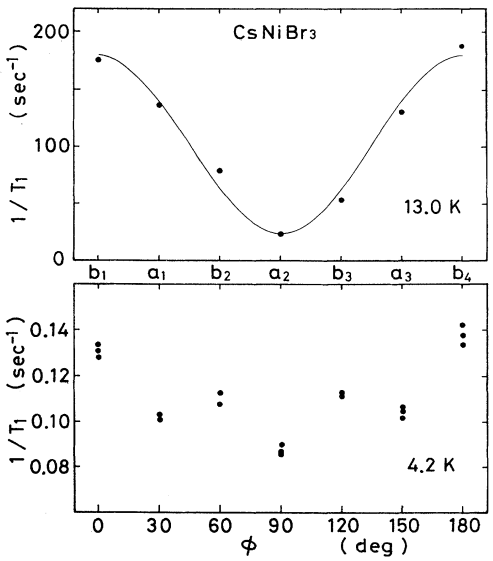


FIG. 2. Peak dependence of the relaxation rate for $\mathbf{H}_0 \perp c$ axis at 13.0 K in the intermediate phase and at 4.2 K in the low-temperature phase. The peaks correspond to the angle $\phi$ between the external field in the $c$ plane and the internal dipolar field at each $^{133}Cs$ site. The solid curve shows the calculated curve of Eq. (2).

is expressed as

$$\frac{1}{T_1}=h_1^2F_1\sin^2\phi+h_2^2F_2\sin^2(90°-\phi)+h_3^2F_3 \quad (2)$$

and the rate for $\mathbf{H}_0\|c$ axis as

$$\frac{1}{T_1}=h_1^2F_1+h_2^2F_2\ , \quad (3)$$

where $F_i$ is the Fourier transform of the normalized correlation function of the fluctuating internal field. The solid curve in Fig. 2 shows the calculated values of Eq. (2) by taking $h_1^2F_1=18$ sec$^{-1}$, $h_2^2F_2=174$ sec$^{-1}$, and $h_3^2F_3=6$ sec$^{-1}$.

We measured $T_1$ also at 2.0 and 7.0 MHz to know the field dependence of the relaxation rate. The central resonance fields at 2.0, 4.0, and 7.0 MHz are 3.6, 7.1, and 12.4 kOe, respectively. The internal field at the Cs sites changed little for the different frequencies. This fact indicates that the spin structure does not deform so much in this field range. The relaxation rates at these frequencies had the same value at each temperature within the experimental error. The relaxation rate at a much higher frequency of 26 MHz whose central resonance field is 46 kOe has been reported previously.[7] Comparing the results, we can conclude that $T_1^{-1}$ is independent of the frequency between 2.0 and 26 MHz or the external field between 3.6 and 46 kOe in all phases.

## IV. ANALYSIS

### A. Paramagnetic phase

The nuclear spin-lattice relaxation rate is calculated from the transition probability between the nuclear spin states by means of first-order perturbation theory. It is generally expressed by the Fourier transform of the time-correlation function of the transverse component $\delta H^{\pm}$ of the fluctuating local field at the nuclear site with respect to the Larmor frequency $\omega_n$ as

$$\frac{1}{T_1}=\frac{\gamma_n^2}{2}\int_{-\infty}^{\infty}dt\langle\{\delta H^-(t)\delta H^+(0)\}\rangle\exp(-i\omega_n t)\ , \quad (4)$$

where $\gamma_n$ is the gyromagnetic ratio of the nuclear spin, $\{AB\}$ denotes the symmetrized product $\frac{1}{2}(AB+BA)$, and $\langle A\rangle$ means the statistical average.

In the paramagnetic phase of this compound the fluctuation of the $Ni^{2+}$ spins due to the exchange interaction causes a fluctuating local field at $^{133}$Cs sites through the dipolar interaction

$$H'=\gamma_e\gamma_n\hbar^2\sum_i\frac{1}{R_i^3}\left\{\mathbf{I}\cdot\mathbf{S}_i-3\frac{(\mathbf{I}\cdot\mathbf{R}_i)(\mathbf{R}_i\cdot\mathbf{S}_i)}{R_i^2}\right\}$$
$$=-\gamma_n\hbar\mathbf{I}\cdot\delta\mathbf{H}\ , \quad (5)$$

where $\gamma_e$ is the gryomagnetic ratio of the electron spin and $\mathbf{R}_i$ is the position vector of the $i$th electron spin $\mathbf{S}_i$ referring to the origin at the nucleus. Then the relaxation rate is given as[8,9]

$$\frac{1}{T_1}=\frac{(\hbar\gamma_e\gamma_n)^2}{4\pi}\int_{-\pi}^{\pi}dq\int_{-\infty}^{\infty}dt\cos(\omega_n t)[\tfrac{1}{4}A^+(q)\langle\{S_q^+(t)S_{-q}^-(0)\}\rangle+A^z(q)\langle\{S_q^z(t)S_{-q}^z(0)\}\rangle]\ , \quad (6)$$

where the geometrical coefficients $A^+(q)$ and $A^z(q)$ are the Fourier transforms of the products of two dipolar interaction tensors, $q$ is a wave vector in the first Brillouin zone, the $z$ axis is along the local field at the nucleus and now parallel to the external field, and

$$S_q^\alpha=N^{-1/2}\sum_i S_i^\alpha\exp(i\mathbf{q}\cdot\mathbf{R}_i)\ . \quad (7)$$

The spin-correlation function is related to the static susceptibility $\chi^\alpha(q)$ and the relaxation function $f_q^\alpha(t)$ owing to the fluctuation-dissipation theorem.[10] By assuming the relaxation function to be an exponential type and taking the high-temperature approximation, we get

$$\frac{1}{T_1}=\frac{\gamma_n^2}{4\pi}kT\int_{-\pi}^{\pi}dq\left[\tfrac{1}{4}A^+(q)\chi^+(q)\frac{2\Gamma_q^+}{\omega_e^2+\Gamma_q^{+2}}+A^z(q)\chi^z(q)\frac{2}{\Gamma_q^z}\right]\ . \quad (8)$$

Here we assume that the quantities in Eq. (8) are $q$ independent. Since the measured relaxation rate is independent of the field, two cases are considered for Eq. (8). One is that only the second term in the integral is dominant. The other case is that the first term is dominant under the condition of $\omega_e\ll\Gamma_q^+$. In any case the temperature dependence of the relaxation rate is given as

$$\frac{1}{T_1}\propto T\chi^\alpha(0)\ . \quad (9)$$

The static susceptibility of $CsNiBr_3$ has been reported by Brener *et al.*,[2] and it has the characteristic temperature dependence of a one-dimensional antiferromagnet with a broad maximum around 40 K and is slightly anisotropic below about 30 K. Using the susceptibility data for $\mathbf{H}_0\perp c$ axis, we calculated the temperature dependence of the relaxation rate by Eq. (9). The calculated values are normalized to be fitted with the data at high temperatures and are shown by a broken curve in Fig. 1. The experimental results and the calculated values agree quite well in the paramagnetic phase.

Generally the critical fluctuation of the $q=\pi$ mode

comes to be dominant near the Néel temperature. This behavior has been clearly demonstrated in a nonfrustrated one-dimensional antiferromagnet $(CH_3)_4NMnCl_3$ (TMMC).[9,11] In $CsNiBr_3$ the experimental data are well explained by the static susceptibility of the $q=0$ mode down to $T_{N1}$. The same behavior has also been observed in $CsNiCl_3$ (Ref. 12) and $RbNiCl_3$ (Ref. 13), which are similar frustrated antiferromagnets on a triangular lattice. This fact may suggest that the critical fluctuation would not develop well due to the frustration effect.

### B. Ordered phases

Next we consider the relaxation time in the low-temperature phase. The strong temperature dependence of the observed relaxation time suggests that the two-magnon (Raman) process is dominant in this phase. The theory of the relaxation time due to the two-magnon process in an antiferromagnet with two magnetic sublattices has been developed by Moriya.[14] For the present case of the triangular-lattice antiferromagnet, the spins form the triangular structure and there are six magnetic sublattices in the low-temperature phase. We extend his theory to the case of the triangular spin structure.

In the ordered phase the fluctuation of the electron spin is

$$\delta\mathbf{S}_i=\mathbf{S}_i-\langle\mathbf{S}_i\rangle\ , \tag{10}$$

and then $\mathbf{S}_i$ in the perturbation of Eq. (5) is replaced by $\delta\mathbf{S}_i$. Since the spins lie in a common plane in the ordered phases, we take this plane as the $zx$ plane with the $z$ axis parallel to the $c$ axis. Next we choose the direction of the local magnetic field at the nucleus as the $z_I$ axis and define the $(x_I,y_I,z_I)$ coordinate system. The direction cosines of these axes are denoted by $(\alpha_1,\beta_1,\gamma_1)$, $(\alpha_2,\beta_2,\gamma_2)$, and $(\alpha,\beta,\gamma)$, and that of the electron-spin position vector $R_i$ by $(\alpha_i,\beta_i,\gamma_i)$. The coordinate systems are illustrated in Fig. 3. Then the relaxation rate is written from Eq. (4) as

$$\frac{1}{T_1}=\gamma_e^2\gamma_n^2\hbar^2\sum_i\sum_j\frac{1}{R_i^3}\frac{1}{R_j^3}\times\int_{-\infty}^{\infty}\{\langle K_i^+(t)K_j^-(0)\rangle e^{i\omega_n t}+\langle K_j^-(t)K_i^+(0)\rangle e^{-i\omega_n t}\}dt\ , \tag{11}$$

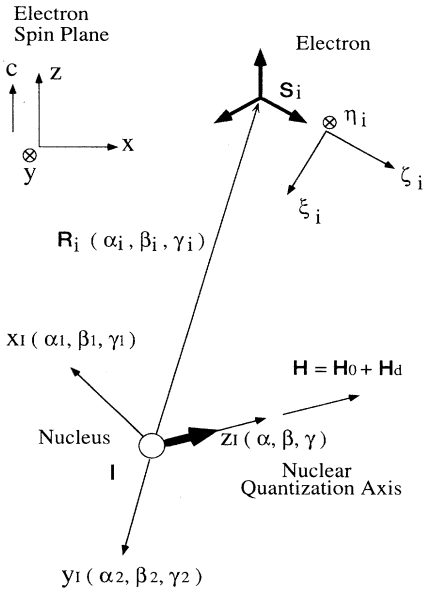


FIG. 3. Coordinate systems for electron spins and nuclear spin in the low-temperature phase. The external magnetic field and static dipolar field at the nuclear site are shown by $\mathbf{H}_0$ and $\mathbf{H}_d$, respectively.

where

$$K_i^{\pm}(t)=\alpha^{\pm}\delta S_{ix}(t)+\beta^{\pm}\delta S_{iy}(t)+\gamma^{\pm}\delta S_{iz}(t)-3(\alpha^{\pm}\alpha_i+\beta^{\pm}\beta_i+\gamma^{\pm}\gamma_i)\times\{\alpha_i\delta S_{ix}(t)+\beta_i\delta S_{iy}(t)+\gamma_i\delta S_{iz}(t)\}\ , \tag{12}$$

$$\alpha^{\pm}=\frac{\alpha_1\pm i\alpha_2}{2},\quad \beta^{\pm}=\frac{\beta_1\pm i\beta_2}{2},\quad \gamma^{\pm}=\frac{\gamma_1\pm i\gamma_2}{2}\ . \tag{13}$$

In the present case, as the nucleus is surrounded by six electron spins with equal distance, the correlations between different spins cannot be neglected. Calculating the correlation of $K_i^{\pm}$, we get from Eq. (11)

$$\frac{1}{T_1}=\tfrac{1}{2}\gamma_e^2\gamma_n^2\hbar^2\sum_i\sum_j\frac{1}{R_i^3}\frac{1}{R_j^3}\left[F_{ij}(\alpha,\beta,\gamma)\int_{-\infty}^{\infty}dt\,\cos\omega_0 t\,\langle\delta S_{iz}(t)\delta S_{jz}(0)\rangle+\tfrac{1}{4}F'_{ij}(\alpha,\beta,\gamma)\int_{-\infty}^{\infty}dt\,\cos\omega_0 t[\langle\delta S_i^+(t)\delta S_j^-(0)\rangle+\langle\delta S_i^-(t)\delta S_j^+(0)\rangle]\right]\ , \tag{14}$$

where

$$F_{ij}(\alpha,\beta,\gamma)=(1-3\gamma_i^2-3\gamma_j^2)(1-\gamma^2)+9\gamma_i\gamma_j(\alpha_i\alpha_j+\beta_i\beta_j+\gamma_i\gamma_j-\alpha_i\alpha_j\alpha^2-\beta_i\beta_j\beta^2-\gamma_i\gamma_j\gamma^2)+3\beta\gamma\{\beta_i\gamma_i+\beta_j\gamma_j-3\gamma_i\gamma_j(\beta_i\gamma_j+\beta_j\gamma_i)\}+3\gamma\alpha\{\gamma_i\alpha_i+\gamma_j\alpha_j-3\gamma_i\gamma_j(\gamma_i\alpha_j+\gamma_j\alpha_i)\}-9\gamma_i\alpha_j\alpha\beta(\alpha_i\beta_j+\alpha_j\beta_i) \tag{15}$$

and $F'_{ij}(\alpha,\beta,\gamma)$ is also the function of the direction cosines.

As the electron spins form a triangular structure in the low-temperature phase, we assume that the spin system takes a helical arrangement with wave vector $\mathbf{Q}$.[15,16] We introduce new rotating coordinate axes $\xi_i$, $\eta_i$, and $\zeta_i$ for each spin, as illustrated in Fig. 3. The $\zeta_i$ axis is taken in the direction parallel to the spin $\mathbf{S}_i$. The $\xi_i$ axis is perpendicular to the $\zeta_i$ axis and in the $zx$ plane. Then the spin correlations in the $(x,y,z)$ system in Eq. (14) are expressed by the components $\delta\hat{S}_{i\xi}$, $\delta\hat{S}_{i\eta}$, and $\delta\hat{S}_{i\zeta}$ in the $(\xi_i,\eta_i,\zeta_i)$ system. The longitudinal correlation is rewritten as

$$\begin{aligned}\langle \delta S_{iz}(t)\delta S_{jz}(0)\rangle =& \tfrac{1}{4}\sin\mathbf{Q}\cdot\mathbf{R}_i \sin\mathbf{Q}\cdot\mathbf{R}_j \\ &\times\{\langle \delta\hat{S}_i^{+}(t)\delta\hat{S}_j^{+}(0)\rangle+\langle \delta\hat{S}_i^{+}(t)\delta\hat{S}_j^{-}(0)\rangle+\langle \delta\hat{S}_i^{-}(t)\delta\hat{S}_j^{+}(0)\rangle+\langle \delta\hat{S}_i^{-}(t)\delta\hat{S}_j^{-}(0)\rangle\} \\ &+\tfrac{1}{2}\sin\mathbf{Q}\cdot\mathbf{R}_i \cos\mathbf{Q}\cdot\mathbf{R}_j\{\langle \delta\hat{S}_i^{+}(t)\delta\hat{S}_{j\zeta}(0)\rangle+\langle \delta\hat{S}_i^{-}(t)\delta\hat{S}_{j\zeta}(0)\rangle\} \\ &+\tfrac{1}{2}\cos\mathbf{Q}\cdot\mathbf{R}_i \sin\mathbf{Q}\cdot\mathbf{R}_j\{\langle \delta\hat{S}_{i\zeta}(t)\delta\hat{S}_j^{+}(0)\rangle+\langle \delta\hat{S}_{i\zeta}(t)\delta\hat{S}_j^{-}(0)\rangle\} \\ &+\cos\mathbf{Q}\cdot\mathbf{R}_i \cos\mathbf{Q}\cdot\mathbf{R}_j\langle \delta\hat{S}_{i\zeta}(t)\delta\hat{S}_{j\zeta}(0)\rangle\ , \end{aligned} \tag{16}$$

where

$$\delta\hat{S}_i^{\pm}=\delta\hat{S}_{i\xi}\pm i\delta\hat{S}_{i\eta}\ . \tag{17}$$

The transverse correlation in Eq. (14) is also written by the sum of spin correlations of $\delta\hat{S}_{i\xi}$, etc. By using the Holstein-Primakoff transform and the Fourier transform, the spin correlations are expressed by the spin-wave annihilation $a_q$ and creation $a_q^*$ operators. The time evolutions of these operators are given by

$$\begin{aligned} a_q(t)&=e^{iH_e t/\hbar}a_q e^{-iH_e t/\hbar}=e^{-i\omega_q t}a_q\ , \\ a_q^*(t)&=e^{iH_e t/\hbar}a_q^* e^{-iH_e t/\hbar}=e^{i\omega_q t}a_q^*\ . \end{aligned} \tag{18}$$

So the correlation function $\langle \delta\hat{S}_{i\zeta}(t)\delta\hat{S}_{j\zeta}(0)\rangle$ has a frequency component corresponding to the frequency difference between two magnons. On the other hand, the other correlation functions contain the same frequency components as the magnon frequency, and therefore contribute to the relaxation due to the direct process. In our case the magnon energy is so large compared to the nuclear Zeeman energy that these correlations do not contribute to the nuclear relaxation. Then the dominant terms of the correlation function for $T_1$ are only

$$\langle \delta S_{iz}(t)\delta S_{jz}(0)\rangle=\cos\mathbf{Q}\cdot\mathbf{R}_i \cos\mathbf{Q}\cdot\mathbf{R}_j\langle \delta\hat{S}_{i\zeta}(t)\delta\hat{S}_{j\zeta}(0)\rangle\ , \tag{19}$$

$$\begin{aligned}&\langle \delta S_i^{+}(t)\delta S_j^{-}(0)\rangle+\langle \delta S_i^{-}(t)\delta S_j^{+}(0)\rangle \\ &\quad=\tfrac{1}{2}\sin\mathbf{Q}\cdot\mathbf{R}_i \sin\mathbf{Q}\cdot\mathbf{R}_j\langle \delta\hat{S}_{i\zeta}(t)\delta\hat{S}_{j\zeta}(0)\rangle\ . \end{aligned} \tag{20}$$

This implies that the fluctuation of the triangular spin structure in the $zx$ plane contributes to the nuclear spin relaxation, because the fluctuation $\delta\hat{S}_{i\zeta}$ comes from the fluctuations $\delta S_{ix}$ and $\delta S_{iz}$.

Then we will consider the temperature dependence of the relaxation time. This comes from the temperature dependence of the correlation $\langle \delta\hat{S}_{i\zeta}(t)\delta\hat{S}_{j\zeta}(0)\rangle$ through the number of magnons. The relaxation rate for the two-magnon process is expressed by[14]

$$\begin{aligned}\frac{1}{T_1}=&\frac{\pi}{2}\gamma_e^2\gamma_n^2\hbar^2\sum_{i,j}G_{ij}\int_{\omega_0}^{\omega_m}\left\{1+\left[\frac{\omega_m}{\omega}\right]^2\right\} \\ &\times\frac{e^{\hbar\omega/kT}}{(e^{\hbar\omega/kT}-1)^2}N(\omega)^2 d\omega\ , \end{aligned} \tag{21}$$

where $G_{ij}$ is the geometrical factor of the dipolar interaction and is related to $F_{ij}(\alpha,\beta,\gamma)$ and $F'_{ij}(\alpha,\beta,\gamma)$, $\omega_m$ is the maximum frequency, and $N(\omega)$ is the state density of magnons. Since the nuclear spin of $^{133}$Cs is located at the center of the unit prism with equal distance from the $Ni^{2+}$ spins, not only the autocorrelation but also the correlation between the different spins must be considered. Here we consider only the temperature dependence of the relaxation time for simplicity.

When the single-ion anisotropy $D$ is zero or negative so that the spins lie in the $c$ plane, the Hamiltonian given by Eq. (1) can be diagonalized within linear spin-wave theory and the magnon excitation energy can be obtained analytically.[15,16] For the present case of a triangular spin structure with the easy-axis anisotropy $D>0$, however, the dispersion relation has not been obtained analytically. The relation has been calculated numerically for the analysis of an inelastic-neutron-scattering experiment, which observed the higher-energy part of the dispersion curve.[17] The nuclear magnetic relaxation is governed by low-energy excitations and thus the dispersion relation at small energy is required to calculate the relaxation time.

Here we apply the long-wave approximation and assume the dispersion relation as

$$\omega=A\{1+Bl^2+C(h^2+k^2)\}^{1/2}\ , \tag{22}$$

where $A$, $B$, and $C$ are constants depending on $J_0$, $J_1$, and $D$, and $h$, $k$, and $l$ are the wave numbers. The state density is calculated from this relation as

$$N(\omega)=\frac{3\omega\sqrt{\omega^2-\omega_0^2}}{(\omega_m^2-\omega_0^2)^{3/2}}\ . \tag{23}$$

Then from Eq. (21) the relaxation rate becomes

$$\frac{1}{T_1}=\frac{\pi}{2}\gamma_e^2\gamma_n^2\hbar^2\sum_{i,j}G_{ij}\frac{9\hbar}{k}\frac{1}{(T_m^2-T_0^2)^3}T^5 \times\int_{T_0/T}^{T_m/T}\left\{x^2-\left[\frac{T_0}{T}\right]^2\right\}\left\{x^2+\left[\frac{T_m}{T}\right]^2\right\}\times\frac{e^x}{(e^x-1)^2}dx\ , \tag{24}$$

where $T_m=\hbar\omega_m/k$ and $T_0=\hbar\omega_0/k$. We took $T_m$ to be 30 K from the dispersion relation observed by the neutron experiment[17] and chose the value of $T_0$ as 2.5 K to fit the experimental results in the lower-temperature region. The calculated temperature dependence of $T_1^{-1}$ is shown by the solid curve in Fig. 1. As seen in Fig. 1, the temperature dependence of the theoretical curve agrees fairly well with the experimental results below about 6 K.

There are three kinds of low-energy excitations in the ordered triangular spin structure.[18,19] The lowest excitation mode corresponds to the rotational fluctuation around the $c$ axis, which is the Goldstone mode. This fluctuation is illustrated in Fig. 4(a). The energy of this mode depends on the magnetic field as

$$\epsilon_1=g\mu_B H_0\ . \tag{25}$$

The second excitation mode corresponds to the swinging fluctuation of the triangular spin structure in the $zx$ plane and is shown in Fig. 4(b). The excitation energy of this mode is independent of the field for $\mathbf{H}_0\perp c$ axis and is nearly independent for $\mathbf{H}_0\|c$ axis.[19] The third excitation mode corresponds to the fluctuation vertical to the $zx$ plane, as shown in Fig. 4(c), and the excitation energy depends on the field.

According to the calculation by Zaliznyak, Prozorova, and Chukukov,[20] the gap energy of the second mode is given as

$$\epsilon_2=\frac{2}{\sqrt{3}}S\left[1-\frac{S}{2}\right]^{3/2}\frac{D}{J_1}\left[J_0D\left[1+\frac{9J_1}{8J_0}\right]\right]^{1/2}. \tag{26}$$

Using the values of $S=1$, $J_0=17.0$ K, $J_1=0.31$ K, and $D=0.65$ K for $CsNiBr_3$, $\epsilon_2$ is estimated to be 2.9 K. On the other hand, Suzuki and Natsume have calculated the energy gap of the swinging fluctuation in the two-dimensional triangular-lattice antiferromagnet with easy-axis anisotropy.[18] Their theory gives $\epsilon_2$ to be 2.2 K for $CsNiBr_3$. Thus the value $T_0$ of 2.5 K that is obtained from our experiment agrees fairly well with the gap energy given by these theories.[18,20]

The energy gaps $\epsilon_1$ of the Goldstone mode in the presence of the magnetic field are estimated to be 0.5, 1.0, and 1.75 K for $\mathbf{H}_0=3.6$, 7.1, and 12.5 kOe, respectively, in our experiments. Though the energy gap $\epsilon_1$ is lower than the energy gap $\epsilon_2$ of the swinging motion, the field-independent relaxation time observed in the low-temperature phase indicates that the Goldstone mode does not contribute to the nuclear relaxation. This fact is consistent with the theoretical calculation mentioned above that the swinging fluctuation in the $zx$ plane contributes to the nuclear relaxation. We conclude that the nuclear spin-lattice relaxation in the low-temperature phase is governed by the two-magnon process related to the swinging fluctuation of the triangular spin structure in the $zx$ plane.

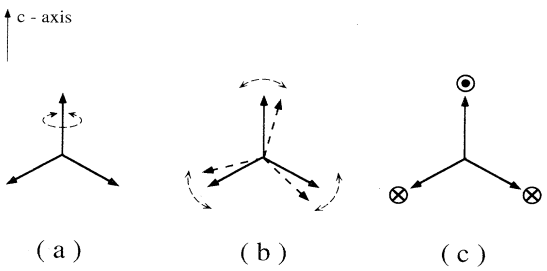


FIG. 4. Spin fluctuations of the triangular spin structure in the low-temperature phase. (a) Rotational fluctuation around the $c$ axis. (b) Swinging fluctuation in the $zx$ plane. (c) Vertical deviation from the $zx$ plane.

## V. DISCUSSION

The experimental results of $T_1^{-1}$ above about 6 K in the low-temperature phase deviate to larger values from the theoretical curve. This deviation may come from the temperature dependence of the dispersion curve. The spins form a triangular configuration in the plane containing the $c$ axis with the fan-out angle of 39° at low enough temperature in the low-temperature phase. As the temperature is raised, the fan-out angle decreases and the transverse component of the magnetic moment becomes smaller. Finally, the fan-out angle and the transverse moment become zero at $T_{N2}$.[3] This is equivalent to the decrease of the effective exchange interaction $J_1$. Thus the energy gap and the energy at the zone boundary would decrease and the slope of the dispersion curve would also decrease, on increasing the temperature. A change of the energy gap has little effect on the temperature dependence of $T_1^{-1}$ in the high-temperature part of the low-temperature phase, as the energy gap 2.5 K is small enough compared to the temperature range concerned. On the other hand, a change of the energy at the zone boundary $T_m$ has a sensitive effect on the temperature dependence of $T_1^{-1}$ in this temperature range. The experimental results of $T_1^{-1}$ can be well fitted by Eq. (24) with the gradual decrease of $T_m$ from $T_m=30$ K below 6 K to $T_m=17$ K at $T_{N2}$. It is worth noting that the temperature above which the observed $T_1^{-1}$ deviates from the calculated curve is nearly equal to the temperature above which the transverse moment begins to shrink.[3]

We could consider another reason for the deviation. As the temperature is raised, the fluctuation of the higher-energy mode would be excited. The next-higher-energy fluctuation is related to the vertical deviation from the $zx$ plane. The energy gap of this mode has been estimated to be about 10 K.[19,20] Thus this fluctuation would be excited around 10 K.

In the intermediate phase the spins form a collinear structure, where the longitudinal component of the moments is ordered but the transverse component is paramagnetic. The observed relaxation rate in this phase has a stronger dependence on both temperature and site than that in the lower-temperature phase. Some excitation modes would contribute to the relaxation rate and the components of the fluctuation at the nuclear sites should be considered. The analysis of the relaxation rate in this partially disordered phase is a problem for the future.

The isomorphic compound $CsNiCl_3$ has been studied by neutron-scattering experiments because of interest in the Haldane gap system, since the compound is a quasi-one-dimensional antiferromagnet with $S=1$.[21,22] These reports claim that the observed spin-wave dispersion shows even in the ordered phase the characteristic behavior that must be attributed to the Haldane effect. One of the purposes of the present experiment was to detect phenomena concerned with the Haldane gap, but no experimental results that should be attributed to the Haldane gap were found.

## VI. SUMMARY

We have measured the spin-lattice relaxation time of $^{133}Cs$ in $CsNiBr_3$, which is a Heisenberg antiferromagnet with easy-axis anisotropy on a triangular lattice. The relaxation rate in the paramagnetic phase above $T_{N1}$ is controlled by the paramagnetic modulation of the exchange interaction. It is well explained by Moriya's theory and is related to the susceptibility through the fluctuation-dissipation theorem. The temperature dependence of the relaxation rate is well fitted by using the observed static susceptibility down to $T_{N1}$. This suggests that the critical fluctuation does not become effective down to $T_{N1}$. This would be one of the characteristic properties due to the frustration effect in a triangular-lattice antiferromagnet. In the low-temperature phase we found that the two-magnon (Raman) process due to the swinging fluctuation of the triangular spin configuration in the $zx$ plane gives the dominant contribution to the relaxation rate and that this mode has the energy gap of 2.5 K independent of the field. The temperature dependence of the observed relaxation rates below about 6 K is well explained by this model. The observed rates above about 6 K in the low-temperature phase deviate from the calculated curve. This deviation coincides with the decrease of the transverse moment. It might be attributed to the gradual decrease of the slope of the dispersion curve and to the contribution of the excitation modes with higher energy. The relaxation mechanism in the intermediate phase remains as a future problem.

## ACKNOWLEDGMENTS

We would like to thank Professor H. Tanaka and Professor K. Iio for providing us the sample for this experiment. We also thank Professor T. Goto, Professor S. Miyashita, and Professor M. Chiba for valuable discussions. This work was partially supported by a Grant-in-Aid for Scientific Research from the Ministry of Education, Science and Culture.

[1]G. D. Stucky, S. D'Agostino, and G. L. McPherson, J. Am. Chem. Soc. **88**, 4828 (1966).
[2]R. Brener, E. Ehrenfreund, H. Shechter, and J. Makovsky, J. Phys. Chem. Solids **38**, 1023 (1977).
[3]S. Maegawa, T. Kohmoto, T. Goto, and N. Fujiwara, Phys. Rev. B **44**, 12 617 (1991).
[4]H. Aruga Katori, T. Goto, and Y. Ajiro, J. Phys. Soc. Jpn. **62**, 743 (1993).
[5]H. Tanaka, J. Magn. Magn. Mater. **90-91**, 251 (1990).
[6]S. Maegawa, T. Goto, and Y. Ajiro, J. Phys. Soc. Jpn. **57**, 1402 (1988).
[7]M. Chiba, Y. Ajiro, H. Kikuchi, S. Maegawa, and T. Morimoto, J. Phys. Soc. Jpn. **61**, 1758 (1992).
[8]T. Moriya, Prog. Theor. Phys. **28**, 371 (1962).
[9]D. Hone, C. Scherer, and F. Borsa, Phys. Rev. B **9**, 965 (1974).
[10]R. Kubo, J. Phys. Soc. Jpn. **12**, 570 (1957).
[11]D. Hone and A. Pires, Phys. Rev. B **15**, 323 (1977).
[12]S. Maegawa (unpublished).
[13]S. Muneta, S. Maegawa, A. Oyamada, T. Goto, and Y. Oohara, in J. Magn. Magn. Mater. **140-144**, 1787 (1995).
[14]T. Moriya, Prog. Theor. Phys. **16**, 23 (1956).
[15]K. Yoshida and H. Miwa, J. Appl. Phys. **32**, 8S (1961).
[16]T. Ohyama and H. Shiba, J. Phys. Soc. Jpn. **62**, 3277 (1993).
[17]R. M. Morra, W. J. L. Buyers, R. L. Armstrong, and K. Hirakawa, Phys. Rev. B **38**, 543 (1988).
[18]T. Suzuki and Y. Natsume, J. Phys. Soc. Jpn. **56**, 1577 (1987).
[19]H. Tanaka, S. Teraoka, E. Kakehashi, K. Iio, and K. Nagata, J. Phys. Soc. Jpn. **57**, 3979 (1988).
[20]I. A. Zaliznyak, L. A. Prozorova, and A. V. Chukukov, J. Phys. Condens. Matter **1**, 4743 (1989).
[21]K. Kakurai, M. Steiner, J. K. Kjems, D. Petitgrand, R. Pynn, and K. Hirakawa, J. Phys. (Paris) Colloq. **T49**, C8-1433 (1988).
[22]Z. Tun, W. J. L. Buyer, R. L. Armstrong, K. Hirakawa, and B. Briat, Phys. Rev. B **42**, 4677 (1990).